



# SINGLE INCLUSIVE DISTRIBUTION AND TWO-PARTICLE CORRELATIONS INSIDE ONE JET AT "MODIFIED LEADING LOGARITHMIC APPROXIMATION" OF QUANTUM CHROMODYNAMICS II: STEEPEST DESCENT EVALUATION AT SMALL X

Redamy Perez Ramos

## ► To cite this version:

Redamy Perez Ramos. SINGLE INCLUSIVE DISTRIBUTION AND TWO-PARTICLE CORRELATIONS INSIDE ONE JET AT "MODIFIED LEADING LOGARITHMIC APPROXIMATION" OF QUANTUM CHROMODYNAMICS II: STEEPEST DESCENT EVALUATION AT SMALL X. Journal of High Energy Physics, 2006, 09, pp.014. hal-00086880

**HAL Id: hal-00086880**

**<https://hal.science/hal-00086880>**

Submitted on 20 Jul 2006

**HAL** is a multi-disciplinary open access archive for the deposit and dissemination of scientific research documents, whether they are published or not. The documents may come from teaching and research institutions in France or abroad, or from public or private research centers.

L'archive ouverte pluridisciplinaire **HAL**, est destinée au dépôt et à la diffusion de documents scientifiques de niveau recherche, publiés ou non, émanant des établissements d'enseignement et de recherche français ou étrangers, des laboratoires publics ou privés.

July 2006

**SINGLE INCLUSIVE DISTRIBUTION AND TWO-PARTICLE CORRELATIONS INSIDE ONE JET  
AT “MODIFIED LEADING LOGARITHMIC APPROXIMATION” OF QUANTUM CHROMODYNAMICS  
II : STEEPEST DESCENT EVALUATION AT SMALL  $x$**

Redamy Perez-Ramos <sup>1</sup>

*Laboratoire de Physique Théorique et Hautes Energies <sup>2</sup>*

*Unité Mixte de Recherche UMR 7589*

*Université Pierre et Marie Curie-Paris6; CNRS; Université Denis Diderot-Paris7*

**Abstract:** The MLLA single inclusive distribution inside one high energy (gluon) jet at small  $x$  is estimated by the steepest descent method. Its analytical expression is obtained outside the “limiting spectrum”. It is then used to evaluate 2-particle correlations at the same level of generality. The dependence of both observables on the ratio between the infrared cutoff  $Q_0$  and  $\Lambda_{QCD}$  is studied. Fong & Webber’s results for correlations are recovered at the limits when this ratio goes to 1 and when one stays close to the peak of the single inclusive distribution.

**Keywords:** *Perturbative Quantum Chromodynamics, Particle Correlations in jets, High Energy Colliders*

---

<sup>1</sup>E-mail: perez@lpthe.jussieu.fr

<sup>2</sup>LPTHE, tour 24-25, 5<sup>ème</sup> étage, Université P. et M. Curie, BP 126, 4 place Jussieu, F-75252 Paris Cedex 05 (France)

# Contents

<b>1</b>	<b>INTRODUCTION</b>	<b>2</b>
<b>2</b>	<b>STEEPEST DESCENT EVALUATION OF THE SINGLE INCLUSIVE DISTRIBUTION</b>	<b>2</b>
2.1	Variables and kinematics . . . . .	2
2.2	Evolution equations for particle spectra at MLLA . . . . .	2
2.3	Evolution equations; steepest descent evaluation . . . . .	3
2.3.1	Shape of the spectrum given in eq. (18) . . . . .	5
2.4	Logarithmic derivatives . . . . .	6
2.4.1	“Limiting spectrum”: $\lambda \rightarrow 0$ ( $Q_0 = \Lambda_{QCD}$ ) . . . . .	8
<b>3</b>	<b>2-PARTICLE CORRELATIONS INSIDE ONE JET AT <math>\lambda \neq 0</math> (<math>Q_0 \neq \Lambda_{QCD}</math>)</b>	<b>8</b>
3.1	Variables and kinematics . . . . .	9
3.2	MLLA evolution equations for correlations . . . . .	9
3.3	MLLA solution at $\lambda \neq 0$ . . . . .	9
3.3.1	Gluon jet . . . . .	10
3.3.2	Quark jet . . . . .	11
3.4	Sensitivity of the quark and gluon jets correlators to the value of $\lambda$ . . . . .	11
3.5	Extension of the Fong and Webber expansion; its limit $\lambda = 0$ . . . . .	13
3.6	Comparison with the exact solution of the evolution equations: $\lambda = 0$ . . . . .	14
3.7	Comparison with Fong-Webber and LEP-I data; how $\lambda = 0$ is favored . . . . .	15
<b>4</b>	<b>CONCLUSION</b>	<b>15</b>
<b>A</b>	<b>DOUBLE DERIVATIVES AND DETERMINANT</b>	<b>17</b>
A.1	Demonstration of eq. (19) . . . . .	17
A.2	$Det A$ (see eq. (19)) around the maximum . . . . .	18
A.3	The functions $L(\mu, v)$ , $K(\mu, v)$ in eq. (26) . . . . .	18
A.4	A consistency check . . . . .	18
<b>B</b>	<b>ANALYTICAL EXPRESSION OF <math>\Delta'(\mu_1, \mu_2)</math> OBTAINED FROM EQ. (41)</b>	<b>20</b>

# 1 INTRODUCTION

Exactly solving the MLLA evolution equations for the quark and gluon inclusive spectra and for 2-particle correlations inside one jet provided, at small  $x$ , in [1], analytical expressions for these observables, which were unfortunately limited, for technical reasons to the “limiting spectrum”  $\lambda \equiv \ln(Q_0/\Lambda_{QCD}) = 0$ . The goal of this second work is to go beyond this limit in an approximate scheme which proves very economical and powerful: the steepest descent (SD) method. It offers sizable technical progress in the calculation of both observables.

First, we perform a SD evaluation of the (quark and) gluon single inclusive distributions. Their full dependence on  $\lambda$  is given, including the normalization. The well known shift to smaller values of  $x$  of the maximum of the distribution, as compared with DLA calculations is checked, as well as its Gaussian shape around the maximum. Comparison with the results obtained numerically in [2] is done.

As shown in [1], knowing the logarithmic derivatives of the inclusive spectra immediately gives access to 2-particle correlations. This is accordingly our next step. Since, in particular, the former prove to be infra-red stable in the limit  $\lambda \rightarrow 0$ , the result can be safely compared with the exact one obtained in [1]. The agreement turns out to be excellent, and increases with the energy scale of the process.

Last, we evaluate 2-particle correlations inside one high energy jet and study their behavior at  $Q_0 \neq \Lambda_{QCD}$ . That one recovers the results of Fong & Webber [3] close to the peak of the single inclusive distribution and when  $\lambda \rightarrow 0$  is an important test of the validity and efficiency of the SD method. The quantitative predictions do not substantially differ from the ones of [1] for the “limiting spectrum”, which stays the best candidate to reproduce experimental results.

A conclusion summarizes the achievements, limitations and expectations of [1] and of the present work. It is completed with two technical appendices.

## 2 STEEPEST DESCENT EVALUATION OF THE SINGLE INCLUSIVE DISTRIBUTION

We consider the production of one hadron inside a quark or a gluon jet in a hard process. It carries the fraction  $x$  of the total energy  $E$  of the jet.  $\Theta_0$  is the half opening angle of the jet while  $\Theta$  is the angle corresponding to the first splitting with energy fraction  $x \ll z \ll 1$ .

### 2.1 Variables and kinematics

The variables and kinematics of the process under consideration are the same as in section 3.1 of [1].

### 2.2 Evolution equations for particle spectra at MLLA

We define like in [1] the logarithmic parton densities

$$Q(\ell) \equiv x D_Q(x), \quad G(\ell) = x D_G(x)$$

for quark and gluon jets in terms of which the system of evolution equations for particle spectra at small  $x$  (see eqs. (42) and (43) of [1]) read

$$Q(\ell, y) = \delta(\ell) + \frac{C_F}{N_c} \int_0^\ell d\ell' \int_0^y dy' \gamma_0^2(\ell' + y') \left(1 - \frac{3}{4} \delta(\ell' - \ell)\right) G(\ell', y'), \quad (1)$$

$$G(\ell, y) = \delta(\ell) + \int_0^\ell d\ell' \int_0^y dy' \gamma_0^2(\ell' + y') \left(1 - a \delta(\ell' - \ell)\right) G(\ell', y'), \quad (2)$$

where

$$a = \frac{1}{4N_c} \left[ \frac{11}{3} N_c + \frac{4}{3} n_f T_R \left( 1 - \frac{2C_F}{N_c} \right) \right] \stackrel{n_f=3}{=} 0.935. \quad (3)$$

The terms  $\propto \frac{3}{4}$  in (1) and  $\propto a$  in (2) account for hard corrections to soft gluon multiplication, sub-leading  $g \rightarrow q\bar{q}$  splittings, strict angular ordering and energy conservation.

### 2.3 Evolution equations; steepest descent evaluation

The exact solution of (2) is demonstrated in [1] to be given by the Mellin's integral representation

$$\begin{aligned} G(\ell, y) &= (\ell + y + \lambda) \iint \frac{d\omega d\nu}{(2\pi i)^2} e^{\omega\ell + \nu y} \int_0^\infty \frac{ds}{\nu + s} \left( \frac{\omega(\nu + s)}{(\omega + s)\nu} \right)^{1/\beta(\omega - \nu)} \left( \frac{\nu}{\nu + s} \right)^{a/\beta} e^{-\lambda s} \\ &= (\ell + y + \lambda) \iint \frac{d\omega d\nu}{(2\pi i)^2} e^{\omega\ell + \nu y} \int_0^\infty \frac{ds}{\nu + s} \left( \frac{\nu}{\nu + s} \right)^{a/\beta} e^{\sigma(s)}, \end{aligned} \quad (4)$$

where we have exponentiated the kernel (symmetrical in  $(\omega, \nu)$ )

$$\sigma(s) = \frac{1}{\beta(\omega - \nu)} \ln \left( \frac{\omega(\nu + s)}{\nu(\omega + s)} \right) - \lambda s. \quad (5)$$

(4) will be estimated by the SD method. The value  $s_0$  of the saddle point, satisfying  $\left. \frac{d\sigma(s)}{ds} \right|_{s=s_0} = 0$ , reads (see [7])

$$s_0(\omega, \nu) = \frac{1}{2} \left[ \sqrt{\frac{4}{\beta\lambda} + (\omega - \nu)^2} - (\omega + \nu) \right]. \quad (6)$$

One makes a Taylor expansion of  $\sigma(s)$  nearby  $s_0$ :

$$\sigma(s) = \sigma(s_0) + \frac{1}{2} \sigma''(s_0) (s - s_0)^2 + \mathcal{O}((s - s_0)^3), \quad \sigma''(s_0) = -\beta\lambda^2 \sqrt{\frac{4}{\beta\lambda} + (\omega - \nu)^2} < 0, \quad (7)$$

such that

$$\int_0^\infty \frac{ds}{\nu + s} \left( \frac{\omega(\nu + s)}{(\omega + s)\nu} \right)^{1/\beta(\omega - \nu)} \left( \frac{\nu}{\nu + s} \right)^{a/\beta} e^{-\lambda s} \stackrel{\lambda \gg 1}{\approx} 2\sqrt{\frac{\pi}{2}} \frac{e^{\sigma(s_0)}}{(\nu + s_0)\sqrt{|\sigma''(s_0)|}} \left( \frac{\nu}{\nu + s_0} \right)^{a/\beta}. \quad (8)$$

The condition  $\lambda \gg 1 \Rightarrow \alpha_s/\pi \ll 1$ <sup>3</sup> guarantees, in particular, the convergence of the perturbative approach. Substituting (8) in (4) yields

$$G(\ell, y) \approx 2\sqrt{\frac{\pi}{2}} (\ell + y + \lambda) \iint \frac{d\omega d\nu}{(2\pi i)^2} \frac{e^{\phi(\omega, \nu, \ell, y)}}{(\nu + s_0)\sqrt{|\sigma''(s_0)|}} \left( \frac{\nu}{\nu + s_0} \right)^{a/\beta}, \quad (9)$$

where the argument of the exponential is

$$\phi(\omega, \nu, \ell, y) = \omega\ell + \nu y + \frac{1}{\beta(\omega - \nu)} \ln \frac{\omega(\nu + s_0)}{(\omega + s_0)\nu} - \lambda s_0. \quad (10)$$

---

<sup>3</sup>in (7),  $\lambda$  appears to the power  $3/2 > 1$ , which guarantees the fast convergence of the SD as  $\lambda$  increases.

Once again, we perform the SD method to evaluate (9). The saddle point  $(\omega_0, \nu_0)$  satisfies the equations

$$\frac{\partial \phi}{\partial \omega} = \ell - \frac{1}{\beta (\omega - \nu)^2} \ln \frac{\omega (\nu + s_0)}{(\omega + s_0) \nu} + \frac{1}{\beta \nu (\omega - \nu)} - \lambda \frac{(\nu + s_0)}{(\omega - \nu)} = 0, \quad (11a)$$

$$\frac{\partial \phi}{\partial \nu} = y + \frac{1}{\beta (\omega - \nu)^2} \ln \frac{\omega (\nu + s_0)}{(\omega + s_0) \nu} - \frac{1}{\beta \nu (\omega - \nu)} + \lambda \frac{(\omega + s_0)}{(\omega - \nu)} = 0. \quad (11b)$$

Adding and subtracting (11a) and (11b) gives respectively

$$\omega_0 \nu_0 = \frac{1}{\beta (\ell + y + \lambda)}, \quad (12a)$$

$$y - \ell = \frac{1}{\beta (\omega_0 - \nu_0)} \left( \frac{1}{\omega_0} + \frac{1}{\nu_0} \right) - \frac{2}{\beta (\omega_0 - \nu_0)^2} \ln \frac{\omega_0 (\nu_0 + s_0)}{(\omega_0 + s_0) \nu_0} - \lambda \frac{\omega_0 + \nu_0 + 2s_0}{\omega_0 - \nu_0}; \quad (12b)$$

$(\omega_0, \nu_0)$  also satisfies (from (6))

$$(\omega_0 + s_0) (\nu_0 + s_0) = \frac{1}{\beta \lambda}. \quad (13)$$

One can substitute the expressions (11a) and (11b) of  $\ell$  and  $y$  into (10), which yields

$$\varphi \equiv \phi(\omega_0, \nu_0, \ell, y) = \frac{2}{\beta (\omega_0 - \nu_0)} \ln \frac{\omega_0 (\nu_0 + s_0)}{(\omega_0 + s_0) \nu_0}. \quad (14)$$

Introducing the variables  $(\mu, v)$  [7] to parametrize  $(\omega_0, \nu_0)$  through

$$\omega_0 (\nu_0) = \frac{1}{\sqrt{\beta (\ell + y + \lambda)}} e^{\pm \mu (\ell, y)}, \quad (\omega_0 + s_0) (\nu_0 + s_0) = \frac{1}{\sqrt{\beta \lambda}} e^{\pm v (\ell, y)}, \quad (15)$$

one rewrites (14) and (12b) respectively in the form

$$\varphi(\mu, v) = \frac{2}{\sqrt{\beta}} \left( \sqrt{\ell + y + \lambda} - \sqrt{\lambda} \right) \frac{\mu - v}{\sinh \mu - \sinh v}, \quad (16)$$

$$\frac{y - \ell}{y + \ell} = \frac{(\sinh 2\mu - 2\mu) - (\sinh 2v - 2v)}{2 (\sinh^2 \mu - \sinh^2 v)}; \quad (17a)$$

moreover, since  $\omega_0 - \nu_0 = (\omega_0 - s_0) - (\nu_0 - s_0)$ ,  $(\mu, v)$  also satisfy

$$\frac{\sinh v}{\sqrt{\lambda}} = \frac{\sinh \mu}{\sqrt{\ell + y + \lambda}}. \quad (17b)$$

Performing a Taylor expansion of  $\phi(\omega, \nu, \ell, y)$  around  $(\omega_0, \nu_0)$ , which needs evaluating  $\frac{\partial^2 \phi}{\partial \omega^2}$ ,  $\frac{\partial^2 \phi}{\partial \nu^2}$  and  $\frac{\partial^2 \phi}{\partial \omega \partial \nu}$  (see appendix A.1), treating  $(Y + \lambda)$  as a large parameter and making use of (15) provides the SD result

$$G(\ell, y) \approx \mathcal{N}(\mu, v, \lambda) \exp \left[ \frac{2}{\sqrt{\beta}} \left( \sqrt{\ell + y + \lambda} - \sqrt{\lambda} \right) \frac{\mu - v}{\sinh \mu - \sinh v} + v - \frac{a}{\beta} (\mu - v) \right], \quad (18)$$

where

$$\mathcal{N}(\mu, v, \lambda) = \frac{1}{2} (\ell + y + \lambda) \frac{\left( \frac{\beta}{\lambda} \right)^{1/4}}{\sqrt{\pi \cosh v \text{Det} A(\mu, v)}} \left( \frac{\lambda}{\ell + y + \lambda} \right)^{a/2\beta}$$

with (see details in appendix A.1)

$$DetA(\mu, \nu) = \beta (\ell + y + \lambda)^3 \left[ \frac{(\mu - \nu) \cosh \mu \cosh \nu + \cosh \mu \sinh \nu - \sinh \mu \cosh \nu}{\sinh^3 \mu \cosh \nu} \right]. \quad (19)$$

### 2.3.1 Shape of the spectrum given in eq. (18)

We normalize (18) by the MLLA mean multiplicity inside one jet [8]

$$\bar{n}(Y) \stackrel{\lambda \gg 1}{\approx} \frac{1}{2} \left( \frac{Y + \lambda}{\lambda} \right)^{-\frac{1}{2} \frac{a}{\beta} + \frac{1}{4}} \exp \left[ \frac{2}{\sqrt{\beta}} \left( \sqrt{Y + \lambda} - \sqrt{\lambda} \right) \right].$$

The normalized expression for the single inclusive distribution as a function of  $\ell = \ln(1/x)$  is accordingly obtained by setting  $y = Y - \ell$  in (18)

$$\frac{G(\ell, Y)}{\bar{n}(Y)} \approx \sqrt{\frac{\beta^{1/2} (Y + \lambda)^{3/2}}{\pi \cosh \nu DetA(\mu, \nu)}} \exp \left[ \frac{2}{\sqrt{\beta}} \left( \sqrt{Y + \lambda} - \sqrt{\lambda} \right) \left( \frac{\mu - \nu}{\sinh \mu - \sinh \nu} - 1 \right) + \nu - \frac{a}{\beta} (\mu - \nu) \right]. \quad (20)$$

One can explicitly verify that (20) preserves the position of the maximum [8][9][10] at

$$\ell_{max} = \frac{Y}{2} + \frac{1}{2} \frac{a}{\beta} \left( \sqrt{Y + \lambda} - \sqrt{\lambda} \right) > \frac{Y}{2}, \quad (21)$$

as well as the gaussian shape of the distribution around (21) (see appendix A.2)

$$\frac{G(\ell, Y)}{\bar{n}(Y)} \approx \left( \frac{3}{\pi \sqrt{\beta} [(Y + \lambda)^{3/2} - \lambda^{3/2}]} \right)^{1/2} \exp \left( -\frac{2}{\sqrt{\beta}} \frac{3}{(Y + \lambda)^{3/2} - \lambda^{3/2}} \frac{(\ell - \ell_{max})^2}{2} \right). \quad (22)$$

In Fig.1 we compare for  $Y = 10$  and  $\lambda = 2.5$  the MLLA curve with DLA (by setting  $a = 0$  in (20)). The general features of the MLLA curve (20) at  $\lambda \neq 0$  are in good agreement with those of [2].

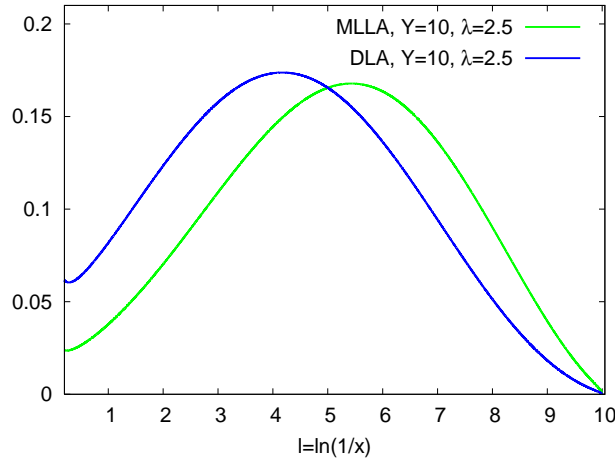


Figure 1: SD normalized spectrum: DLA (blue), MLLA (green);  $Y = 10.0$ ,  $\lambda = 2.5$ .

The shape of the single inclusive spectrum given by (20) can easily be proved to be “infrared stable” (it has indeed a final limit when  $\lambda \rightarrow 0$ ).

## 2.4 Logarithmic derivatives

Their calculation is important since they appear in the expressions of 2-particle correlations.

Exponentiating the  $(\ell, y)$  dependence of the factor  $\mathcal{N}$  in (18), we decompose the whole expression in two pieces

$$\psi = \varphi + \delta\psi, \quad (23)$$

where  $\varphi$ , given in (16), is the DLA term for the shape of the distribution [7], and

$$\delta\psi = -\frac{1}{2} \left(1 + \frac{a}{\beta}\right) \ln(\ell + y + \lambda) - \frac{a}{\beta} \mu + \left(1 + \frac{a}{\beta}\right) v + \frac{1}{2} \ln[Q(\mu, v)] \quad (24)$$

is the sub-leading contribution (in the sense that its derivative gives the MLLA correction), where

$$Q(\mu, v) \equiv \frac{\beta(\ell + y + \lambda)^3}{\cosh v \text{Det } A(\mu, v)} = \frac{\sinh^3 \mu}{(\mu - v) \cosh \mu \cosh v + \cosh \mu \sinh v - \sinh \mu \cosh v}.$$

By the definition of the saddle point, the derivatives of (16) over  $\ell$  and  $y$  respectively read:

$$\varphi_\ell = \omega_0 = \gamma_0 e^\mu, \quad \varphi_y = \nu_0 = \gamma_0 e^{-\mu}. \quad (25)$$

We introduce (see appendix A.3)

$$\begin{aligned} \mathcal{L}(\mu, v) &= -\frac{a}{\beta} + L(\mu, v), & L(\mu, v) &= \frac{1}{2} \frac{\partial}{\partial \mu} \ln[Q(\mu, v)], \\ \mathcal{K}(\mu, v) &= 1 + \frac{a}{\beta} + K(\mu, v), & K(\mu, v) &= \frac{1}{2} \frac{\partial}{\partial v} \ln[Q(\mu, v)] \end{aligned} \quad (26)$$

and make use of

$$\frac{\partial v}{\partial \ell} = \tanh v \left( \coth \mu \frac{\partial \mu}{\partial \ell} - \frac{1}{2} \beta \gamma_0^2 \right), \quad \frac{\partial v}{\partial y} = \tanh v \left( \coth \mu \frac{\partial \mu}{\partial y} - \frac{1}{2} \beta \gamma_0^2 \right),$$

that follows from (17b), to write  $\delta\psi_\ell$ ,  $\delta\psi_y$  in terms of  $\frac{\partial \mu}{\partial \ell}$ ,  $\frac{\partial \mu}{\partial y}$

$$\delta\psi_\ell = -\frac{1}{2} \left(1 + \frac{a}{\beta} + \tanh v \mathcal{K}(\mu, v)\right) \beta \gamma_0^2 + \left(\mathcal{L}(\mu, v) + \tanh v \coth \mu \mathcal{K}(\mu, v)\right) \frac{\partial \mu}{\partial \ell}, \quad (27a)$$

$$\delta\psi_y = -\frac{1}{2} \left(1 + \frac{a}{\beta} + \tanh v \mathcal{K}(\mu, v)\right) \beta \gamma_0^2 + \left(\mathcal{L}(\mu, v) + \tanh v \coth \mu \mathcal{K}(\mu, v)\right) \frac{\partial \mu}{\partial y}. \quad (27b)$$

Using (17a) and (17b) we obtain

$$\frac{\partial \mu}{\partial \ell} = -\frac{1}{2} \beta \gamma_0^2 \left[1 + e^\mu \tilde{Q}(\mu, v)\right], \quad \frac{\partial \mu}{\partial y} = \frac{1}{2} \beta \gamma_0^2 \left[1 + e^{-\mu} \tilde{Q}(\mu, v)\right] \quad (28)$$

where

$$\tilde{Q}(\mu, v) = \frac{\cosh \mu \sinh \mu \cosh v - (\mu - v) \cosh v - \sinh v}{(\mu - v) \cosh \mu \cosh v + \cosh \mu \sinh v - \sinh \mu \cosh v}, \quad (29)$$

which we have displayed in Fig.2 (useful for correlations).



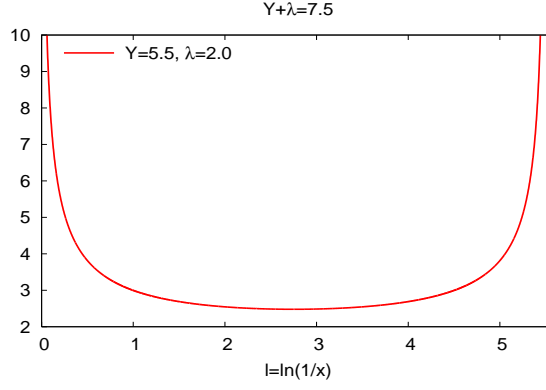


Figure 2: Behavior of  $\tilde{Q}(\mu, v)$  as a function of  $\ell = \ln(1/x)$ .

Inserting (27b) and (28) into (27a) gives the SD logarithmic derivatives of the single inclusive distribution

$$\begin{aligned} \psi_\ell(\mu, v) = & \gamma_0 e^\mu + \frac{1}{2} a \gamma_0^2 \left[ e^\mu \tilde{Q}(\mu, v) - \tanh v - \tanh v \coth \mu \left( 1 + e^\mu \tilde{Q}(\mu, v) \right) \right] \\ & - \frac{1}{2} \beta \gamma_0^2 \left[ 1 + \tanh v \left( 1 + K(\mu, v) \right) + C(\mu, v) \left( 1 + e^\mu \tilde{Q}(\mu, v) \right) \right] + \mathcal{O}(\gamma_0^2), \end{aligned} \quad (30a)$$

$$\begin{aligned} \psi_y(\mu, v) = & \gamma_0 e^{-\mu} - \frac{1}{2} a \gamma_0^2 \left[ 2 + e^{-\mu} \tilde{Q}(\mu, v) + \tanh v - \tanh v \coth \mu \left( 1 + e^{-\mu} \tilde{Q}(\mu, v) \right) \right] \\ & - \frac{1}{2} \beta \gamma_0^2 \left[ 1 + \tanh v \left( 1 + K(\mu, v) \right) - C(\mu, v) \left( 1 + e^{-\mu} \tilde{Q}(\mu, v) \right) \right] + \mathcal{O}(\gamma_0^2) \end{aligned} \quad (30b)$$

where we have introduced ( $L$  and  $K$  have been written in (67) and (68))

$$C(\mu, v) = L(\mu, v) + \tanh v \coth \mu \left( 1 + K(\mu, v) \right). \quad (31)$$

$C$  does not diverge when  $\mu \sim v \rightarrow 0$ . One has indeed

$$\lim_{\mu, v \rightarrow 0} [L(\mu, v) + \tanh v \coth \mu K(\mu, v)] = \lim_{\mu, v \rightarrow 0} \frac{2 - 3 \frac{v^2}{\mu^2} - \frac{v^3}{\mu^3}}{4 \left( 1 - \frac{v^3}{\mu^3} \right)} \mu = 0$$

as well as

$$\lim_{\mu, v \rightarrow 0} \tanh v \coth \mu \left( 1 + e^{\pm \mu} \tilde{Q}(\mu, v) \right) = \lim_{\mu, v \rightarrow 0} \frac{3 \frac{v}{\mu}}{1 - \frac{v^3}{\mu^3}} = \frac{3 \sqrt{\frac{\lambda}{Y+\lambda}}}{1 - \left( \frac{\lambda}{Y+\lambda} \right)^{3/2}}.$$

In (30a) and (30b) it is easy to keep trace of leading and sub-leading contributions. The first  $\mathcal{O}(\gamma_0)$  term is DLA [7] while the second ( $\propto a \rightarrow$  “hard corrections”) and third ( $\propto \beta \rightarrow$  “running coupling effects”) terms are MLLA corrections ( $\mathcal{O}(\gamma_0^2)$ ), of relative order  $\mathcal{O}(\gamma_0)$  with respect to the leading one. In Fig.3 we plot (30a) (left) and (30b) (right) for two different values of  $\lambda$ ; one observes that  $\psi_\ell$  ( $\psi_y$ ) decreases (increases) when  $\lambda$  increases.

For further use in correlations, the logarithmic derivatives have the important property that they do not depend on the normalization but only on the shape of the single inclusive distribution.

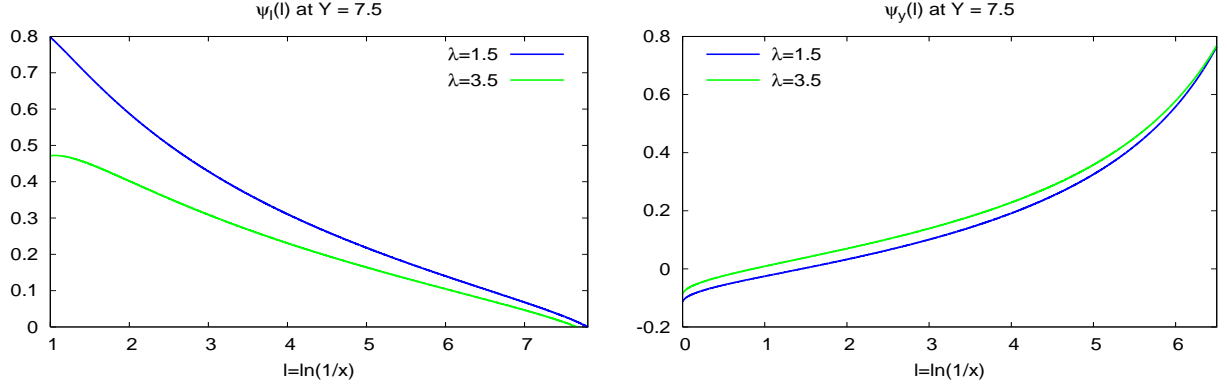


Figure 3: SD logarithmic derivatives  $\psi_\ell$  and  $\psi_y$  of the inclusive spectrum at  $Y = 7.5$ , for  $\lambda = 1.5$  and  $\lambda = 3.5$ .

#### 2.4.1 “Limiting spectrum”: $\lambda \rightarrow 0$ ( $Q_0 = \Lambda_{QCD}$ )

Since the logarithmic derivatives are “infrared stable” (see above), we can take the limit  $\lambda \rightarrow 0$  in (30a)(30b)<sup>4</sup>, and compare their shapes with the ones obtained in [5]; this is done in Figs. 4 and 5, at LEP-I energy ( $E\Theta_0 = 91.2$  GeV,  $Y = 5.2$ ) and at the unrealistic value  $Y = 15$ .

The agreement between the SD and the exact logarithmic derivatives is seen to be quite good. The small deviations ( $\leq 20\%$ ) that can be observed at large  $\ell$  (the domain we deal with) arise from NMLLA corrections that one does not control in the exact solution. The agreement gets better and better as the energy increases.

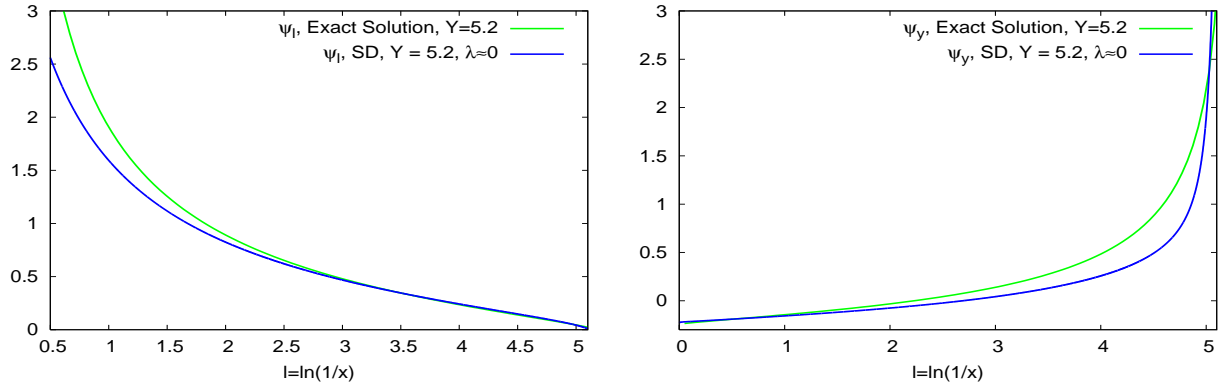


Figure 4: SD logarithmic derivatives  $\psi_\ell$  (left) and  $\psi_y$  (right) compared with the ones of [1] at  $Y = 5.2$ .

It is checked in appendix (A.4) that (18) satisfies the evolution equation (2); the SD logarithmic derivatives (30a) and (30b) can therefore be used in the approximate calculation of 2-particle correlations at  $\lambda \neq 0$ . This is what is done in the next section.

### 3 2-PARTICLE CORRELATIONS INSIDE ONE JET AT $\lambda \neq 0$ ( $Q_0 \neq \Lambda_{QCD}$ )

We study the correlation between 2-particles inside one jet of half opening angle  $\Theta$  within the MLLA accuracy. They have fixed energies  $x_1 = \omega_1/E$ ,  $x_2 = \omega_2/E$  ( $\omega_1 > \omega_2$ ) and are emitted at arbitrary

<sup>4</sup>For this purpose, (17a) has been numerically inverted.

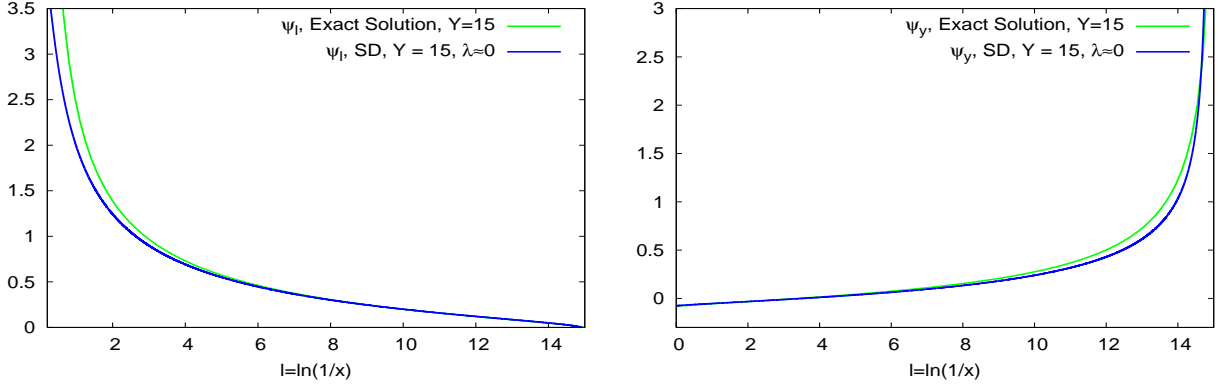


Figure 5: SD logarithmic derivatives  $\psi_\ell$  (left) and  $\psi_y$  (right) compared with the ones of [1] at  $Y = 15$ .

angles  $\Theta_1, \Theta_2$ . The constrain  $\Theta_1 \geq \Theta_2$  follows from the angular ordering in the cascading process. One has  $\Theta \geq \Theta_1$  (see Fig. 1 of [1]).

### 3.1 Variables and kinematics

The variables and kinematics of the cascading process are defined like in section 3.2 of [1].

### 3.2 MLLA evolution equations for correlations

The system of integral evolution equations for the quark and gluon jets two-particle correlation reads (see eqs. (65) and (66) of [1])

$$Q^{(2)}(\ell_1, y_2, \eta) - Q_1(\ell_1, y_1)Q_2(\ell_2, y_2) = \frac{C_F}{N_c} \int_0^{\ell_1} d\ell \int_0^{y_2} dy \gamma_0^2(\ell + y) \left[ 1 - \frac{3}{4} \delta(\ell - \ell_1) \right] G^{(2)}(\ell, y, \eta), \quad (32)$$

$$\begin{aligned} G^{(2)}(\ell_1, y_2, \eta) - G_1(\ell_1, y_1)G_2(\ell_2, y_2) = & \int_0^{\ell_1} d\ell \int_0^{y_2} dy \gamma_0^2(\ell + y) \left[ 1 - a\delta(\ell - \ell_1) \right] G^{(2)}(\ell, y, \eta) \\ & + (a - b) \int_0^{y_2} dy \gamma_0^2(\ell_1 + y) G(\ell_1, y + \eta) G(\ell_1 + \eta, y). \end{aligned} \quad (33)$$

$a$  is defined in (3) while

$$b = \frac{1}{4N_c} \left[ \frac{11}{3} N_c - \frac{4}{3} n_f T_R \left( 1 - 2 \frac{C_F}{N_c} \right)^2 \right]_{n_f=3} \approx 0.915. \quad (34)$$

### 3.3 MLLA solution at $\lambda \neq 0$

The quark and gluon jet correlators  $\mathcal{C}_q$  and  $\mathcal{C}_g$  have been exactly determined for any  $\lambda$  in [1] by respectively setting  $Q^{(2)} = \mathcal{C}_q Q_1 Q_2$  and  $G^{(2)} = \mathcal{C}_g G_1 G_2$  into (32) and (33). In the present work we limit ourselves to the exact MLLA solution which consists in neglecting all  $\mathcal{O}(\gamma_0^2)$  corrections in equations (64) and (84) of [1].

### 3.3.1 Gluon jet

At MLLA, the logarithmic derivatives of  $\psi$  (23) can be truncated to the saddle point derivatives  $\varphi_\ell$ ,  $\varphi_y$  of (16). The MLLA solution of (33) then reads (see (77) in [1])

$$C_g - 1 \stackrel{MLLA}{\approx} \frac{1 - b(\varphi_{1,\ell} + \varphi_{2,\ell}) - \delta_1}{1 + \bar{\Delta} + \Delta' + \delta_1} \quad (35)$$

where we introduce

$$\bar{\Delta} = \gamma_0^{-2} \left( \varphi_{1,\ell} \varphi_{2,y} + \varphi_{1,y} \varphi_{2,\ell} \right), \quad (36)$$

$$\Delta' = \gamma_0^{-2} \left( \varphi_{1,\ell} \delta \psi_{2,y} + \delta \psi_{1,y} \varphi_{2,\ell} + \delta \psi_{1,\ell} \varphi_{2,y} + \varphi_{1,y} \delta \psi_{2,\ell} \right); \quad (37)$$

$$\chi = \ln \left( 1 + \frac{1}{1 + \bar{\Delta}} \right), \quad \chi_\ell = \frac{1}{\chi} \frac{\partial \chi}{\partial \ell}, \quad \chi_y = \frac{1}{\chi} \frac{\partial \chi}{\partial y}; \quad (38)$$

$$\delta_1 = \gamma_0^{-2} \left[ \chi_\ell (\varphi_{1,y} + \varphi_{2,y}) + \chi_y (\varphi_{1,\ell} + \varphi_{2,\ell}) \right]. \quad (39)$$

(36) is obtained by using (25):

$$\bar{\Delta}(\mu_1, \mu_2) = 2 \cosh(\mu_1 - \mu_2) = \mathcal{O}(1), \quad (40)$$

which is the DLA contribution [7], while (37) (see appendix B) is obtained by using (25), (27a) and (27b)

$$\Delta'(\mu_1, \mu_2) = \frac{e^{-\mu_1} \delta \psi_{2,\ell} + e^{-\mu_2} \delta \psi_{1,\ell} + e^{\mu_1} \delta \psi_{2,y} + e^{\mu_2} \delta \psi_{1,y}}{\gamma_0} = \mathcal{O}(\gamma_0); \quad (41)$$

it is a next-to-leading (MLLA) correction. To get (38), we first use (40), which gives

$$\chi_\ell = -\frac{\tanh \frac{\mu_1 - \mu_2}{2}}{1 + 2 \cosh(\mu_1 - \mu_2)} \left( \frac{\partial \mu_1}{\partial \ell} - \frac{\partial \mu_2}{\partial \ell} \right), \quad \chi_y = -\frac{\tanh \frac{\mu_1 - \mu_2}{2}}{1 + 2 \cosh(\mu_1 - \mu_2)} \left( \frac{\partial \mu_1}{\partial y} - \frac{\partial \mu_2}{\partial y} \right), \quad (42)$$

and then (28) to get

$$\chi_\ell = \beta \gamma_0^2 \frac{\tanh \frac{\mu_1 - \mu_2}{2}}{1 + 2 \cosh(\mu_1 - \mu_2)} \frac{e^{\mu_1} \tilde{Q}_1 - e^{\mu_2} \tilde{Q}_2}{2}, \quad \chi_y = -\beta \gamma_0^2 \frac{\tanh \frac{\mu_1 - \mu_2}{2}}{1 + 2 \cosh(\mu_1 - \mu_2)} \frac{e^{-\mu_1} \tilde{Q}_1 - e^{-\mu_2} \tilde{Q}_2}{2}$$

which are  $\mathcal{O}(\gamma_0^2)$ . They should be plugged into (39) together with (25), which gives

$$\delta_1 = \beta \gamma_0 \frac{2 \sinh^2 \left( \frac{\mu_1 - \mu_2}{2} \right)}{3 + 4 \sinh^2 \left( \frac{\mu_1 - \mu_2}{2} \right)} \left( \tilde{Q}(\mu_1, v_1) + \tilde{Q}(\mu_2, v_2) \right) = \mathcal{O}(\gamma_0); \quad (43)$$

it is also a MLLA term. For  $Q \gg Q_0 \geq \Lambda_{QCD}$  we finally get,

$$C_g(\ell_1, \ell_2, Y, \lambda) \stackrel{MLLA}{\approx} 1 + \frac{1 - b \gamma_0 (e^{\mu_1} + e^{\mu_2}) - \delta_1}{1 + 2 \cosh(\mu_1 - \mu_2) + \Delta'(\mu_1, \mu_2) + \delta_1} \quad (44)$$

where the expression for  $\Delta'$  (74) is written in appendix B. It is important to notice that  $\delta_1 \simeq 0$  near  $\ell_1 \approx \ell_2$  ( $\mu_1 \approx \mu_2$ ) while it is positive and increases as  $\eta$  gets larger (see (29) and Fig.2); it makes the correlation function narrower in  $|\ell_1 - \ell_2|$ .

### 3.3.2 Quark jet

The MLLA solution of (32) reads (see (93) in [1])

$$\frac{C_q - 1}{C_g - 1} \stackrel{MLLA}{\approx} \frac{N_c}{C_F} \left[ 1 + (b - a)(\phi_{1,\ell} + \phi_{2,\ell}) \frac{1 + \bar{\Delta}}{2 + \bar{\Delta}} \right] \quad (45)$$

Inserting (36)-(39) into (45) we get

$$C_q(\ell_1, \ell_2, Y, \lambda) \stackrel{MLLA}{\approx} 1 + \frac{N_c}{C_F} \left( C_g(\ell_1, \ell_2, Y, \lambda) - 1 \right) \left[ 1 + (b - a) \gamma_0 (e^{\mu_1} + e^{\mu_2}) \frac{1 + 2 \cosh(\mu_1 - \mu_2)}{2 + 2 \cosh(\mu_1 - \mu_2)} \right].$$

which finally reduces (for  $Q \gg Q_0 \geq \Lambda_{QCD}$ ) to

$$C_q(\ell_1, \ell_2, Y, \lambda) \stackrel{MLLA}{\approx} 1 + \frac{N_c}{C_F} \left[ \left( C_g(\ell_1, \ell_2, Y, \lambda) - 1 \right) + \frac{1}{2} (b - a) \gamma_0 \frac{e^{\mu_1} + e^{\mu_2}}{1 + \cosh(\mu_1 - \mu_2)} \right]. \quad (46)$$

### 3.4 Sensitivity of the quark and gluon jets correlators to the value of $\lambda$

Increasing  $\lambda$  translates into taking the limits  $\beta, \Lambda_{QCD} \rightarrow 0$  ( $Y = \ell + y \ll \lambda$ ,  $Q \gg Q_0 \gg \Lambda_{QCD}$ ) in the definition of the anomalous dimension via the running coupling constant ( $\gamma_0 = \gamma_0(\alpha_s)$ , see (44) in [1]). It allows to neglect  $\ell, y$  with respect to  $\lambda$  as follows

$$\gamma_0^2(\ell + y) = \frac{1}{\beta(\ell + y + \lambda)} \stackrel{\ell+y \ll \lambda}{\approx} \gamma_0^2 = \frac{1}{\beta\lambda}, \quad (47)$$

such that  $\gamma_0$  can be taken as a constant. Estimating (4) in the region  $\lambda \gg 1 \Leftrightarrow s \ll 1$  needs evaluating the kernel

$$\begin{aligned} & \frac{1}{\nu + s} \left( \frac{\omega(\nu + s)}{(\omega + s)\nu} \right)^{1/\beta(\omega - \nu)} \left( \frac{\nu}{\nu + s} \right)^{a/\beta} \stackrel{s \ll 1}{\approx} \frac{1}{\nu} \left( 1 + \frac{\omega - \nu}{\omega\nu} s \right)^{1/\beta(\omega - \nu)} \left( 1 - \frac{s}{\nu} \right)^{a/\beta} \\ & \approx \frac{1}{\nu} \left[ 1 + \frac{1}{\nu} \left( \frac{1}{\omega} - a \right) \frac{s}{\beta} + \frac{1}{2!} \frac{1}{\nu^2} \left( \frac{1}{\omega} - a \right)^2 \frac{s^2}{\beta^2} + \frac{1}{3!} \frac{1}{\nu^3} \left( \frac{1}{\omega} - a \right)^3 \frac{s^3}{\beta^3} + \dots \right]. \end{aligned} \quad (48)$$

Integrating (48) over  $s$ , using (47) and  $\int_0^\infty s^n e^{-\lambda s} = \frac{n!}{\lambda^{n+1}}$ , we get

$$\begin{aligned} \mathcal{G}(\omega, \nu) & \approx \frac{1}{\nu} \left[ 1 + \frac{1}{\nu} \left( \frac{1}{\omega} - a \right) \frac{1}{\beta\lambda} + \frac{1}{\nu^2} \left( \frac{1}{\omega} - a \right)^2 \left( \frac{1}{\beta\lambda} \right)^2 + \frac{1}{\nu^3} \left( \frac{1}{\omega} - a \right)^3 \left( \frac{1}{\beta\lambda} \right)^3 + \dots \right] \\ & = \frac{1}{\nu - \gamma_0^2 (1/\omega - a)}, \end{aligned}$$

which, after inverting the Mellin's representation (132) of [1], gives

$$G(\ell, y) \stackrel{x \ll 1}{\approx} \exp(2\gamma_0 \sqrt{\ell y} - a\gamma_0^2 y). \quad (49)$$

Taking the same limit in (17a) and (17b) gives respectively

$$\frac{y - \ell}{y + \ell} \stackrel{\ell+y \ll \lambda}{\approx} \tanh \mu \Rightarrow \mu = \frac{1}{2} \ln \frac{y}{\ell}, \quad \mu - v \stackrel{\ell+y \ll \lambda}{\approx} \frac{1}{2} \frac{y - \ell}{\lambda} \Rightarrow \mu \sim v. \quad (50)$$

Furthermore, we use (50) to show how (23) reduces to the exponent in (49)<sup>5</sup>

$$\phi = \frac{2}{\sqrt{\beta}} \frac{\mu - v}{\sinh \mu - \sinh v} \stackrel{\ell+y \ll \lambda}{\approx} 2\gamma_0 \sqrt{\ell y},$$

<sup>5</sup>we set  $\beta = 0$  in (30a), (30b) and only consider terms  $\propto a$

$$\left(\frac{\nu_0}{\nu_0 + s_0}\right)^{a/\beta} = -\frac{1}{2}\frac{a}{\beta}\ln\left(1 + \frac{\ell + y}{\lambda}\right) - \frac{a}{\beta}(\mu - \nu) \approx -\frac{1}{2}\frac{a}{\beta}\frac{\ell + y}{\lambda} - \frac{a}{\beta}(\mu - \nu) \quad (51)$$

$$\stackrel{\ell+y \ll \lambda}{\approx} -a\gamma_0^2 y.$$

Thus, since  $\mu = \frac{1}{2}\ln\frac{y}{\ell}$  (50), (30a) and (30b) simplify to

$$\psi_\ell \stackrel{\ell+y \ll \lambda}{\approx} \gamma_0 e^\mu = \gamma_0 \sqrt{\frac{y}{\ell}}, \quad \psi_y \stackrel{\ell+y \ll \lambda}{\approx} \gamma_0 e^{-\mu} - a\gamma_0^2 = \gamma_0 \sqrt{\frac{\ell}{y}} - a\gamma_0^2. \quad (52)$$

Therefore, taking the limit  $\beta, \Lambda_{QCD} \rightarrow 0$  ( $\lambda \rightarrow \infty$ ) leads to the simplified model described in section 4.2 of [1]. Setting, for the sake of simplicity,  $\ell_1 \approx \ell_2$  in (44)(45), where  $\delta_1$  vanishes, we obtain, in the high energy limit

$$\mathcal{C}_g(\ell, y) \simeq 1 + \frac{1}{3} \left[ 1 - 2 \left( b - \frac{1}{3}a \right) \psi_\ell(\ell, y) \right], \quad \mathcal{C}_q(\ell, y) \simeq 1 + \frac{N_c}{C_F} \left[ \frac{1}{3} - \frac{1}{2} \left( \frac{5}{3}a + b \right) \psi_\ell(\ell, y) \right], \quad (53)$$

where

$$b - \frac{1}{3}a = \frac{1}{18} \left( 11 - 8\frac{T_R}{N_c} + 28\frac{T_R}{N_c}\frac{C_F}{N_c} - 24\frac{T_R}{N_c}\frac{C_F^2}{N_c^2} \right) \stackrel{n_f=3}{\approx} 0.6,$$

$$\frac{5}{3}a + b = \frac{2}{9} \left( 11 + \frac{T_R}{N_c} + \frac{T_R}{N_c}\frac{C_F}{N_c} - 6\frac{T_R}{N_c}\frac{C_F^2}{N_c^2} \right) \stackrel{n_f=3}{\approx} 2.5. \quad (54)$$

Thus, when  $\lambda$  increases by decreasing  $\Lambda_{QCD}$ ,  $\psi_\ell \propto \gamma_0$  decreases and the correlators (53) increase. For LHC, a typical value is  $Y = 7.5$  and we compare in Fig. 6, at fixed  $Q_0$ , the limiting case  $\lambda \approx 0$  ( $Q_0 \approx \Lambda_{QCD} \approx 253$  MeV) with  $\lambda \approx 1.0$  ( $\Lambda_{QCD} = 100$  MeV) and  $\lambda \approx 2.3$  ( $\Lambda_{QCD} = 25$  MeV). As predicted by (53), the correlation increases when  $\Lambda_{QCD} \rightarrow 0$  at fixed  $Q_0$ .

It is also sensitive to the value of  $Q_0$ . As seen in (53), since  $y = \ln\frac{Q}{Q_0} - \ell$ , if one increases  $Q_0$  (since  $\Lambda_{QCD}$  is fixed,  $\gamma_0$  does not change), thereby reducing the available phase space, the correlators increase. This dependence of the correlators at fixed  $\Lambda_{QCD}$  is displayed in Fig.7 for  $0.3 \text{ GeV} \leq Q_0 \leq 1.0 \text{ GeV}$  at  $\ell_1 = \ell_2 = 3.0$  (soft parton).

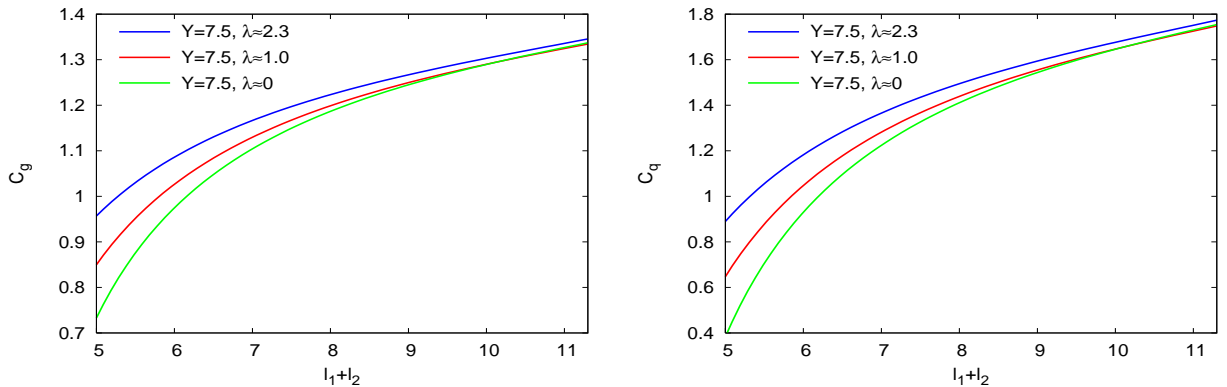


Figure 6: Varying  $\lambda$  at fixed  $Q_0$ ;  $\Lambda_{QCD}$  dependence of  $\mathcal{C}_g$  (left) and  $\mathcal{C}_q$  (right)

In the simplified model which leads to (53),  $\mathcal{C}_g$  and  $\mathcal{C}_q$  respectively go to the asymptotic values  $4/3$  and  $1 + N_c/3C_F$ . This is however not the case in the general situation  $\beta \neq 0$ , as can be easily checked by

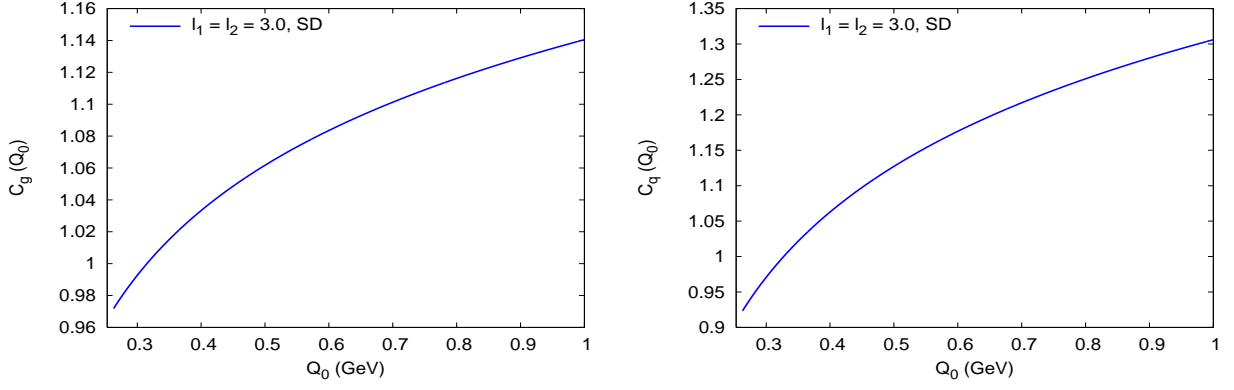


Figure 7: Varying  $\lambda$  at fixed  $\Lambda_{QCD} = 253 \text{ MeV}$ ;  $Q_0$ -dependence of  $C_g$  (left) and  $C_q$  (right) at  $\ell_1 = \ell_2 = 3.0$

using (30a) and (30b); for example, near the maximum of the distribution ( $\mu \sim v \rightarrow 0$ ), a contribution  $\propto \lambda^{3/2}/[(Y + \lambda)^{3/2} - \lambda^{3/2}]$  occurs in the term proportional to  $\beta$  in (53) that yields negative values of  $\psi_\ell$  when  $\lambda$  increases.

### 3.5 Extension of the Fong and Webber expansion; its limit $\lambda = 0$

In the Fong-Webber regime, the energies of the two registered particles stay very close to the peak of the inclusive hump-backed distribution that is,  $|\ell_i - \ell_{max}| \ll \sigma \propto [(Y + \lambda)^{3/2} - \lambda^{3/2}]^{1/2}$  (see (22)).

Near the maximum of the single inclusive distribution  $\ell_1 \sim \ell_2 \simeq Y/2$  ( $\mu, v \rightarrow 0$ , see appendix A.2)

$$\lim_{\mu, v \rightarrow 0} C = \left( \frac{\lambda}{Y + \lambda} \right)^{1/2}, \quad \lim_{\mu, v \rightarrow 0} K_i = \frac{3}{2} \frac{v_i^2}{\mu_i^3 - v_i^3}, \quad \lim_{\mu, v \rightarrow 0} \tilde{Q} = \frac{2}{3} + \frac{1}{3} \left( \frac{\lambda}{Y + \lambda} \right)^{3/2},$$

where  $C$ ,  $K_i$  and  $\tilde{Q}$  are defined in (31), (68) and (29). Keeping only the terms linear in  $\mu$  and the term quadratic in the difference  $(\mu_1 - \mu_2)$ , one has

$$\bar{\Delta} + \Delta' \stackrel{\ell_1 \sim \ell_2 \simeq Y/2}{\simeq} 2 + (\mu_1 - \mu_2)^2 - a\gamma_0(2 + \mu_1 + \mu_2) - \beta\gamma_0 \left[ 2 + 3 \frac{\lambda^{3/2}}{(Y + \lambda)^{3/2} - \lambda^{3/2}} \right] \quad (55)$$

and

$$\delta_1 \stackrel{\ell_1 \sim \ell_2 \simeq Y/2}{\simeq} \frac{1}{9} \beta \gamma_0 (\mu_1 - \mu_2)^2 \left[ 2 + \left( \frac{\lambda}{Y + \lambda} \right)^{3/2} \right]; \quad (56)$$

$\delta_1$  can be neglected, since  $\gamma_0(\mu_1 - \mu_2)^2 \ll (\mu_1 - \mu_2)^2 \ll 1$ . Then, in the same limit, (44), (46) become

$$C_g^0(\ell_1, \ell_2, Y, \lambda) \stackrel{\ell_1 \sim \ell_2 \simeq Y/2}{\simeq} 1 + \frac{1 - b\gamma_0(2 + \mu_1 + \mu_2)}{3 + (\mu_1 - \mu_2)^2 - a\gamma_0(2 + \mu_1 + \mu_2) - \beta\gamma_0 \left[ 2 + 3 \frac{\lambda^{3/2}}{(Y + \lambda)^{3/2} - \lambda^{3/2}} \right]}, \quad (57)$$

$$C_q^0(\ell_1, \ell_2, Y, \lambda) \stackrel{\ell_1 \sim \ell_2 \simeq Y/2}{\simeq} 1 + \frac{N_c}{C_F} \left[ \left( C_g^0(\ell_1, \ell_2, Y, \lambda) - 1 \right) + \frac{1}{4} (b - a) \gamma_0 (2 + \mu_1 + \mu_2) \right]. \quad (58)$$

Using (64) one has

$$(\mu_1 - \mu_2)^2 \simeq 9 \frac{Y + \lambda}{[(Y + \lambda)^{3/2} - \lambda^{3/2}]^2} (\ell_1 - \ell_2)^2, \quad \mu_1 + \mu_2 \simeq 3 \frac{(Y + \lambda)^{1/2}}{(Y + \lambda)^{3/2} - \lambda^{3/2}} [Y - (\ell_1 + \ell_2)]$$

such that the expansion of (57), (58) in  $\gamma_0 \propto \sqrt{\alpha_s}$  reads

$$\begin{aligned} \mathcal{C}_g^0(\ell_1, \ell_2, Y, \lambda) \simeq & \frac{4}{3} - \left( \frac{(Y + \lambda)^{1/2} (\ell_1 - \ell_2)}{(Y + \lambda)^{3/2} - \lambda^{3/2}} \right)^2 + \left( \frac{2}{3} + \frac{(Y + \lambda)^{1/2} Y}{(Y + \lambda)^{3/2} - \lambda^{3/2}} \right) \left( \frac{1}{3} a - b \right) \gamma_0 \\ & + \frac{1}{3} \left( \frac{2}{3} + \frac{\lambda^{3/2}}{(Y + \lambda)^{3/2} - \lambda^{3/2}} \right) \beta \gamma_0 + \left( b - \frac{1}{3} a \right) \left( \frac{(Y + \lambda)^{1/2} (\ell_1 + \ell_2)}{(Y + \lambda)^{3/2} - \lambda^{3/2}} \right) \gamma_0 + \mathcal{O}(\gamma_0^2), \end{aligned} \quad (59)$$

$$\begin{aligned} \mathcal{C}_q^0(\ell_1, \ell_2, Y, \lambda) \simeq & 1 + \frac{N_c}{3C_F} + \frac{N_c}{C_F} \left[ - \left( \frac{(Y + \lambda)^{1/2} (\ell_1 - \ell_2)}{(Y + \lambda)^{3/2} - \lambda^{3/2}} \right)^2 - \frac{1}{4} \left( \frac{2}{3} + \frac{(Y + \lambda)^{1/2} Y}{(Y + \lambda)^{3/2} - \lambda^{3/2}} \right) \left( \frac{5}{3} a + b \right) \gamma_0 \right. \\ & \left. + \frac{1}{3} \left( \frac{2}{3} + \frac{\lambda^{3/2}}{(Y + \lambda)^{3/2} - \lambda^{3/2}} \right) \beta \gamma_0 + \frac{1}{4} \left( \frac{5}{3} a + b \right) \left( \frac{(Y + \lambda)^{1/2} (\ell_1 + \ell_2)}{(Y + \lambda)^{3/2} - \lambda^{3/2}} \right) \gamma_0 \right] + \mathcal{O}(\gamma_0^2). \end{aligned} \quad (60)$$

Therefore, near the hump of the single inclusive distribution, (44), (46) behave as a linear functions of the sum  $(\ell_1 + \ell_2)$  and as a quadratic functions of the difference  $(\ell_1 - \ell_2)$ . At the limit  $\lambda = 0$ , one recovers the Fong-Webber expression [3].

### 3.6 Comparison with the exact solution of the evolution equations: $\lambda = 0$

In Figs.8 we compare the SD evaluation of the gluon correlator with the exact solution of [1] at  $\lambda = 0$ . The difference comes from sub-leading corrections of order  $\gamma_0^2$  that are not present in (44). For example,  $-\beta\gamma_0^2 \approx -0.2$  at  $Y = 5.2$  occurring in the exact solution (69) of [1] is not negligible but is absent in (44) and (46). That is why, the SD MLLA curve lies slightly above the one of [1] at small  $\ell_1 + \ell_2$ . The mismatch becomes smaller at  $Y = 7.5$ , since  $-\beta\gamma_0^2 \approx -0.13$ . However, when  $\ell_1 + \ell_2$  increases, the solution of [1] takes over, which can be explained by comparing the behavior of the SD MLLA  $\delta_1$  obtained in (43) and  $\delta_c, \tilde{\delta}_c$  in [1]. Namely, while  $\delta_1$  remains positive and negligible for  $\ell_1 \approx \ell_2$ ,  $\delta_c, \tilde{\delta}_c$  decrease and get negative when  $\ell_1 + \ell_2 \rightarrow 2Y$ , see Fig.9 (left), which makes the correlations slightly bigger in this region. As  $|\ell_1 - \ell_2|$  increases,  $\delta_1$  is seen in Fig.9 (right) to play the same role as  $\delta_c, \tilde{\delta}_c$  do in the solution [1] and therefore, to decrease the correlation. The agreement between both methods improves as the energy scale increases. A similar behavior holds for the quark correlator.

In [1], strong cancellations between the MLLA  $\delta_1$  and the NMLLA  $\delta_2$  were seen to take place, giving very small  $\delta_c$  and  $\tilde{\delta}_c$ ; this eased the convergence of the iterative method but raised questions concerning the relative size of MLLA and NMLLA corrections and the validity of the perturbative expansion. However, since  $\delta_1$  is itself, there, entangled with *some* NMLLA corrections, no definitive conclusions could be drawn. The present work and Fig. 9, by showing that, below,  $\delta_c$  and  $\tilde{\delta}_c$  of [1] play the same role as the *pure* MLLA  $\delta_1$  which is now calculated, suggests (though it is not a demonstration) that the perturbative series is safe. It is indeed compatible with the following scheme: in [1], the pure MLLA part of  $\delta_1$  is the same as that in the present work; the cancellations in [1] occur between NMLLA corrections included in  $\delta_1$  and  $\delta_2$ ; these are eventually of the same order of magnitude as MLLA terms, but they are only parts of all NMLLA corrections; this leaves the possibility that the sum of all NMLLA corrections to  $\delta_1$  and all NMLLA terms of  $\delta_2$  are separately smaller than the pure MLLA terms of  $\delta_1$ , that is that strong cancellations occur *between NMLLA corrections*, the ones included, because of the logic of the calculation, in [1], and those which were not be taken into account.



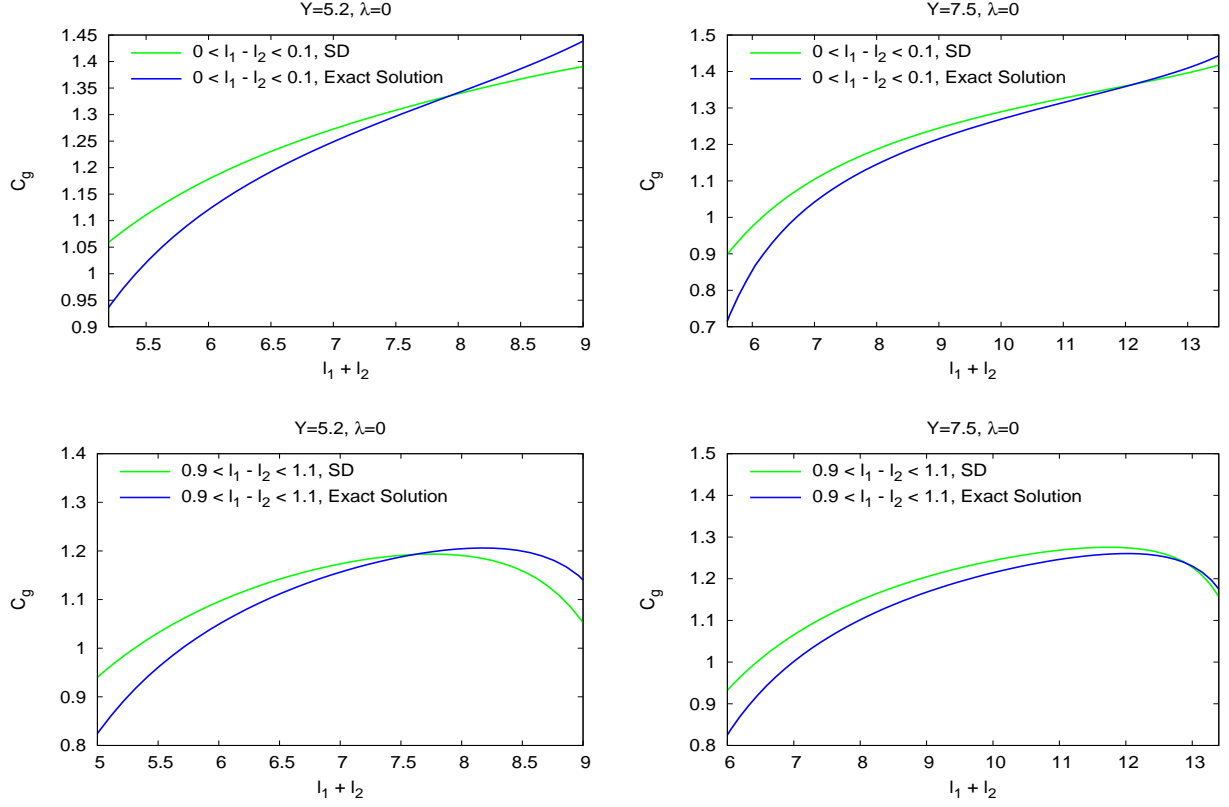


Figure 8: Comparison between correlators given by SD and in [1], at  $\lambda = 0$ .

### 3.7 Comparison with Fong-Webber and LEP-I data; how $\lambda = 0$ is favored

Let us consider, at the  $Z^0$  peak  $Y = 5.2$  ( $E\Theta = 91.2$  GeV at LEP-I energy), the process  $e^+e^- \rightarrow q\bar{q}$ . As can be induced from Fig.8, the results obtained in the present work by the (approximate) SD method are very close to the ones obtained in subsection 6.5 of [1] by the exact solution of the evolution equations. Accordingly, the same comparison as in [1] holds with respect to both Fong & Webber's results [3] and OPAL data [6].

It is also noticeable that, since, at  $\lambda = 0$ , correlations already lie above (present) experimental curves, and since an increase of  $\lambda$  tends to increase the predictions, the limiting spectrum stays the best candidate to bring agreement with experiments.

## 4 CONCLUSION

Let us, in a few words, summarize the achievements, but also the limitations of the two methods that have been used respectively in [1] (exact solution of MLLA evolution equations) and in the present work (steepest descent approximate evaluation of their solutions).

Achievements are threefold:

- in [1], MLLA evolution equations for 2-particle correlations have been deduced at small  $x$  and at any  $\lambda$ ; their (iterative) solution can unfortunately only be expressed analytically at the limit  $\lambda \rightarrow 0$ ;
- by the steepest descent method, which is an approximate method, analytical expressions for the spectrum could instead be obtained for  $\lambda \neq 0$ , which enabled to calculate the correlation at the same level of generality;
- one could move away from the peak of the inclusive distribution.

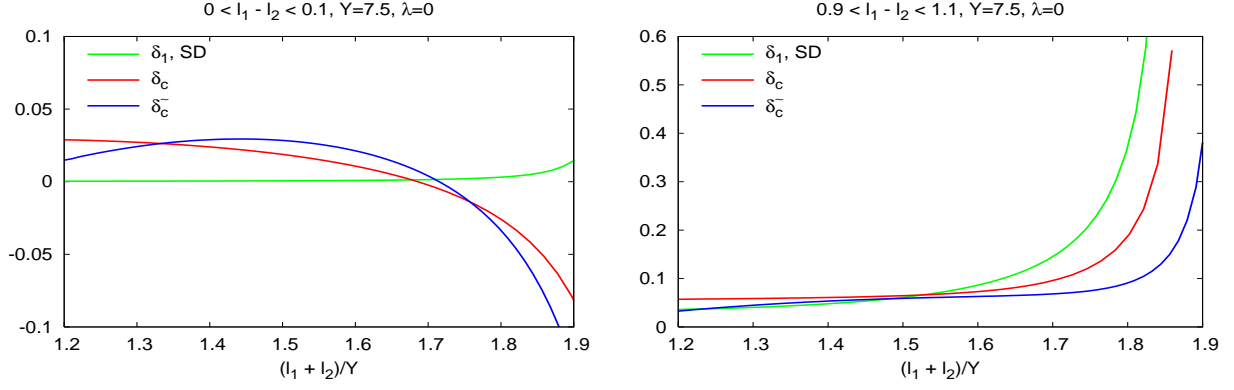


Figure 9: Comparison between the SD  $\delta_1$  and  $\delta_c$ ,  $\tilde{\delta}_c$  of [1] at  $Y = 7.5$ ,  $\lambda = 0$ .

So doing, the limitations of the work of Fong & Webber have vanished. Their results have been recovered at the appropriate limits.

The two methods numerically agree remarkably well, despite an unavoidable entanglement of MLLA + some NMLLA corrections in the first one.

The limitations are the following:

- the uncontrollable increase of  $\alpha_s$  when one goes to smaller and smaller transverse momenta: improvements in this directions mainly concern the inclusion of non-perturbative contributions;
- departure from the limiting spectrum: it cannot of course appear as a limitation, but we have seen that increasing the value of  $\lambda$ , by increasing the correlations, does not bring better agreement with present data; it confirms thus, at present, that the limiting spectrum is the best possibility;
- the LPHD hypothesis: it works surprisingly well for inclusive distributions; only forthcoming data will assert whether its validity decreases when one studies less inclusive processes (like correlations);
- last, the limitation to small  $x$ : it is still quite drastic; departing from this limit most probably lye in the art of numerical calculations, which makes part of forthcoming projects.

Expectations rest on experimental data, which are being collected at the Tevatron, and which will be at LHC. The higher the energy, the safer perturbative QCD is, and the better the agreement should be with our predictions. The remaining disagreement (but much smaller than Fong-Webber's) between predictions and LEP-1 results for 2-particle correlations stands as an open question concerning the validity of the LPHD hypothesis for these observables which are not “so” inclusive as the distributions studied in [5]. The eventual necessity to include NMLLA corrections can only be decided when new data appear.

#### Acknowledgments:

It is a pleasure to thank Yuri Dokshitzer for enticing me towards the steepest descent method and for showing me its efficiency with simple examples. I am grateful to Bruno Machet for his help and advice and to Gavin Salam for helping me in numerically inverting formula (17a).

## A DOUBLE DERIVATIVES AND DETERMINANT

### A.1 Demonstration of eq. (19)

We conveniently rewrite (11a) and (11b) in the form

$$\frac{\partial \phi}{\partial \omega} = \frac{2\omega - \nu}{\omega - \nu} \ell + \frac{\nu}{\omega - \nu} - \frac{\phi}{\omega - \nu} - \lambda \frac{\nu + 2s_0}{\omega - \nu} + \frac{1}{\beta \omega (\omega - \nu)}, \quad (61)$$

$$\frac{\partial \phi}{\partial \nu} = \frac{\omega - 2\nu}{\omega - \nu} y - \frac{\omega}{\omega - \nu} + \frac{\phi}{\omega - \nu} + \lambda \frac{\omega + 2s_0}{\omega - \nu} - \frac{1}{\beta \nu (\omega - \nu)}. \quad (62)$$

The Taylor expansion of (10) in (9) reads

$$\begin{aligned} \phi(\omega, \nu, \ell, y) &\approx \phi(\omega_0, \nu_0, \ell, y) + \frac{1}{2} \frac{\partial^2 \phi}{\partial \omega^2}(\omega_0, \nu_0) (\omega - \omega_0)^2 + \frac{1}{2} \frac{\partial^2 \phi}{\partial \nu^2}(\omega_0, \nu_0) (\nu - \nu_0)^2 \\ &\quad + \frac{\partial^2 \phi}{\partial \omega \partial \nu}(\omega_0, \nu_0) (\omega - \omega_0) (\nu - \nu_0). \end{aligned} \quad (63)$$

The expressions of the second derivatives follow directly from (61) and (62)

$$\frac{\partial^2 \phi}{\partial \omega^2} = -\frac{\nu}{(\omega - \nu)^2} (\ell + y + \lambda) + \frac{\phi}{(\omega - \nu)^2} - \frac{2\omega - \nu}{\beta \omega^2 (\omega - \nu)^2} + \frac{4}{\beta (\omega - \nu)^2 (2s_0 + \omega + \nu)},$$

$$\frac{\partial^2 \phi}{\partial \nu^2} = -\frac{\omega}{(\omega - \nu)^2} (\ell + y + \lambda) + \frac{\phi}{(\omega - \nu)^2} + \frac{\omega - 2\nu}{\beta \nu^2 (\omega - \nu)^2} + \frac{4}{\beta (\omega - \nu)^2 (2s_0 + \omega + \nu)},$$

$$\frac{\partial^2 \phi}{\partial \omega \partial \nu} = \frac{\omega}{(\omega - \nu)^2} (\ell + y + \lambda) - \frac{\phi}{(\omega - \nu)^2} + \frac{1}{\beta \omega (\omega - \nu)^2} - \frac{4}{\beta (\omega - \nu)^2 (2s_0 + \omega + \nu)}.$$

(9) and its solution can be written in the form

$$G \simeq \iint d^2 v e^{-\frac{1}{2} v^T A v} = \frac{2\pi}{\sqrt{\text{Det } A}}$$

where

$$v = (\omega, \nu), \quad v^T = \begin{pmatrix} \omega \\ \nu \end{pmatrix}, \quad \text{Det } A = \text{Det} \begin{pmatrix} \frac{\partial^2 \phi}{\partial \omega^2} & \frac{\partial^2 \phi}{\partial \omega \partial \nu} \\ \frac{\partial^2 \phi}{\partial \nu \partial \omega} & \frac{\partial^2 \phi}{\partial \nu^2} \end{pmatrix} = \frac{\partial^2 \phi}{\partial \omega^2} \frac{\partial^2 \phi}{\partial \nu^2} - \left( \frac{\partial^2 \phi}{\partial \omega \partial \nu} \right)^2.$$

An explicit calculation gives

$$\text{Det } A = (\ell + y + \lambda)^2 \left[ \frac{\beta(\omega + \nu)\phi - 4}{(\omega - \nu)^2} + \frac{4(\omega + \nu)}{(\omega - \nu)^2 (2s_0 + \omega + \nu)} \right]$$

which, by using (15) leads to (19).

## A.2 $DetA$ (see eq. (19)) around the maximum

This is an addendum to subsection 2.3

$\ell_{max}$  written in (21) is close to the DLA value  $Y/2$  [7][8][9]. We then have  $\mu \sim v \rightarrow 0$  for  $\ell \approx y \simeq Y/2$ . In this limit, (17a) and (17b) respectively translate into

$$Y - 2\ell \stackrel{\mu, v \rightarrow 0}{\approx} \frac{2}{3} \frac{(Y + \lambda)^{3/2} - \lambda^{3/2}}{(Y + \lambda)^{1/2}} \mu, \quad v \stackrel{\mu, v \rightarrow 0}{\approx} \sqrt{\frac{\lambda}{Y + \lambda}} \mu, \quad (64)$$

while

$$\frac{\partial \mu}{\partial \ell} \simeq -3 \frac{(Y + \lambda)^{1/2}}{(Y + \lambda)^{3/2} - \lambda^{3/2}} \quad (65)$$

should be used to get (22). An explicit calculation gives

$$\lim_{\mu, v \rightarrow 0} \sqrt{\frac{\beta^{1/2} (Y + \lambda)^{3/2}}{\pi DetA(\mu, v)}} = \left( \frac{3}{\pi \sqrt{\beta} [(Y + \lambda)^{3/2} - \lambda^{3/2}]} \right)^{1/2},$$

where

$$\begin{aligned} DetA &\stackrel{\mu, v \rightarrow 0}{\approx} \beta(Y + \lambda)^3 \frac{(\mu - v) \left(1 + \frac{1}{2}\mu^2\right) \left(1 + \frac{1}{2}v^2\right) + \left(1 + \frac{1}{2}\mu^2\right) \left(v + \frac{1}{6}v^3\right) - \left(\mu + \frac{1}{6}\mu^3\right) \left(1 + \frac{1}{2}v^2\right)}{\mu^3} \\ &\simeq \frac{1}{3} \beta(Y + \lambda)^3 \left(1 - \frac{v^3}{\mu^3}\right) = \frac{1}{3} \beta(Y + \lambda)^3 \left[1 - \left(\frac{\lambda}{Y + \lambda}\right)^{3/2}\right]. \end{aligned} \quad (66)$$

## A.3 The functions $L(\mu, v)$ , $K(\mu, v)$ in eq. (26)

An explicit calculation gives

$$L(\mu, v) = \frac{3}{2} \frac{\cosh \mu}{\sinh \mu} - \frac{1}{2} \frac{(\mu - v) \cosh v \sinh \mu + \sinh v \sinh \mu}{(\mu - v) \cosh \mu \cosh v + \cosh \mu \sinh v - \sinh \mu \cosh v}, \quad (67)$$

and

$$K(\mu, v) = -\frac{1}{2} \sinh v \frac{(\mu - v) \cosh \mu - \sinh \mu}{(\mu - v) \cosh \mu \cosh v + \cosh \mu \sinh v - \sinh \mu \cosh v}. \quad (68)$$

## A.4 A consistency check

Let us verify that the evolution equation (2) is satisfied by (20) within the MLLA accuracy. Differentiating (2) with respect to  $\ell$ ,  $y$  yields the equivalent differential equation

$$G_{\ell y} = \gamma_0^2 (G - a G_\ell) + \mathcal{O}(\gamma_0^4 G)$$

that can be rewritten in the form

$$\psi_\ell \psi_y + \psi_{\ell y} = \gamma_0^2 (1 - a \psi_\ell) + \mathcal{O}(\gamma_0^4); \quad (69)$$

we have neglected next-to-MLLA corrections  $\mathcal{O}(\gamma_0^4)$  (of relative order  $\gamma_0^2$ ) coming from differentiating the coupling  $\gamma_0^2$  in the sub-leading (“hard correction”) term  $\propto a$ .

We have to make sure that (69) holds including the terms  $\mathcal{O}(\gamma_0^3)$ . In the sub-leading terms we can set  $\psi \rightarrow \varphi$  (see (25)):

$$(\varphi_\ell + \delta\psi_\ell)(\varphi_y + \delta\psi_y) + \varphi_{\ell y} = \gamma_0^2(1 - a\varphi_\ell). \quad (70)$$

Isolating correction terms and casting them all on the l.h.s. of the equation we get

$$a\gamma_0^2\varphi_\ell + [\varphi_\ell\delta\psi_y + \varphi_y\delta\psi_\ell] + \varphi_{\ell y} = \gamma_0^2 - \varphi_\ell\varphi_y. \quad (71)$$

By the definition (25) of the saddle point we conclude that the r.h.s. of (71) is zero such that we have

$$\omega_0 a\gamma_0^2 + [\omega_0\delta\psi_y + \nu_0\delta\psi_\ell] + \frac{d\omega_0}{dy} = 0, \quad (72)$$

that is,

$$\omega_0 (a\gamma_0^2 + \delta\psi_y) + \nu_0\delta\psi_\ell + \frac{d\omega_0}{dy} = 0. \quad (73)$$

First, we select the terms  $\propto a$ :

$$\begin{aligned} & a\gamma_0^3 \left[ -\frac{1}{2}\tilde{Q} - \frac{1}{2}\tanh v e^\mu + \frac{1}{2}\tanh v \coth \mu e^\mu + \frac{1}{2}\tanh v \coth \mu \tilde{Q} \right. \\ & \left. + \frac{1}{2}\tilde{Q} - \frac{1}{2}\tanh v e^{-\mu} - \frac{1}{2}\tanh v \coth \mu e^{-\mu} - \frac{1}{2}\tanh v \coth \mu \tilde{Q} \right] \\ & = a\gamma_0^3 [-\tanh v \cosh \mu + \tanh v \coth \mu \sinh \mu] \equiv 0. \end{aligned}$$

From (15) one deduces

$$\frac{d\omega_0}{dy} = \frac{1}{2}\beta\gamma_0^3\tilde{Q},$$

that is inserted in (73) such that, for terms  $\propto \beta$ , we have

$$\begin{aligned} & -\beta\gamma_0^3 \left[ \frac{1}{2}e^\mu + \frac{1}{2}\tanh v (1+K)e^\mu - \frac{1}{2}C e^\mu - \frac{1}{2}C\tilde{Q} + \frac{1}{2}e^{-\mu} + \frac{1}{2}\tanh v (1+K)e^{-\mu} \right. \\ & \left. + \frac{1}{2}C e^{-\mu} + \frac{1}{2}C\tilde{Q} \right] = -\beta\gamma_0^3 \left[ \cosh \mu + \tanh v \cosh \mu (1+K) - C \sinh \mu - \frac{1}{2}\tilde{Q} \right], \end{aligned}$$

which gives

$$-\beta\gamma_0^3 \left[ \cosh \mu - \sinh \mu L - \frac{1}{2}\tilde{Q} \right].$$

Constructing (see (29) and appendix A.3)

$$\begin{aligned} \tilde{Q}(\mu, v) - 2 \cosh \mu &= -3 \cosh \mu + \sinh \mu \frac{(\mu - v) \cosh v \sinh \mu + \sinh v \sinh \mu}{(\mu - v) \cosh \mu \cosh v + \cosh \mu \sinh v - \sinh \mu \cosh v} \\ &= -2 \sinh \mu L(\mu, v) \end{aligned}$$

we have

$$-\beta\gamma_0^3 \left[ \cosh \mu - \sinh \mu L - \frac{1}{2}\tilde{Q} \right] \equiv 0.$$

## B ANALYTICAL EXPRESSION OF $\Delta'(\mu_1, \mu_2)$ OBTAINED FROM EQ. (41)

Replacing (30a)(30b) in (41) and neglecting terms of relative order  $\mathcal{O}(\gamma_0^3)$  which are beyond the MLLA accuracy, we obtain

$$\begin{aligned}
\Delta' &= \frac{e^{-\mu_1} \delta \psi_{2,\ell} + e^{-\mu_2} \delta \psi_{1,\ell} + e^{\mu_1} \delta \psi_{2,y} + e^{\mu_2} \delta \psi_{1,y}}{\gamma_0} \\
&= -a\gamma_0 \left[ e^{\mu_1} + e^{\mu_2} - \sinh(\mu_1 - \mu_2)(\tilde{Q}_1 - \tilde{Q}_2) + \cosh \mu_1 \tanh v_2 + \cosh \mu_2 \tanh v_1 \right. \\
&\quad \left. - \sinh \mu_1 \tanh v_2 \coth \mu_2 - \sinh \mu_2 \tanh v_1 \coth \mu_1 \right. \\
&\quad \left. + \sinh(\mu_1 - \mu_2) \left( \tanh v_1 \coth \mu_1 \tilde{Q}_1 - \tanh v_2 \coth \mu_2 \tilde{Q}_2 \right) \right] \\
&\quad - \beta\gamma_0 \left[ \left( \cosh \mu_1 - \sinh \mu_1 C_2 \right) + \left( \cosh \mu_2 - \sinh \mu_2 C_1 \right) + \sinh(\mu_1 - \mu_2)(C_1 \tilde{Q}_1 - C_2 \tilde{Q}_2) \right. \\
&\quad \left. + \cosh \mu_1 \tanh v_2 (1 + K_2) + \cosh \mu_2 \tanh v_1 (1 + K_1) \right]. \tag{74}
\end{aligned}$$

## List of Figures

1	SD normalized spectrum: DLA (blue), MLLA (green); $Y = 10.0, \lambda = 2.5$ . . . . .	5
2	Behavior of $\tilde{Q}(\mu, v)$ as a function of $\ell = \ln(1/x)$ . . . . .	7
3	SD logarithmic derivatives $\psi_\ell$ and $\psi_y$ of the inclusive spectrum at $Y = 7.5$ , for $\lambda = 1.5$ and $\lambda = 3.5$ . . . . .	8
4	SD logarithmic derivatives $\psi_\ell$ (left) and $\psi_y$ (right) compared with the ones of [1] at $Y = 5.2$ . . . . .	8
5	SD logarithmic derivatives $\psi_\ell$ (left) and $\psi_y$ (right) compared with the ones of [1] at $Y = 15$ . . . . .	9
6	Varying $\lambda$ at fixed $Q_0$ ; $\Lambda_{QCD}$ dependence of $\mathcal{C}_g$ (left) and $\mathcal{C}_q$ (right) . . . . .	12
7	Varying $\lambda$ at fixed $\Lambda_{QCD} = 253 \text{ MeV}$ ; $Q_0$ -dependence of $\mathcal{C}_g$ (left) and $\mathcal{C}_q$ (right) at $\ell_1 = \ell_2 = 3.0$ . . . . .	13
8	Comparison between correlators given by SD and in [1], at $\lambda = 0$ . . . . .	15
9	Comparison between the SD $\delta_1$ and $\delta_c, \tilde{\delta}_c$ of [1] at $Y = 7.5, \lambda = 0$ . . . . .	16

## References

- [1] R. Perez-Ramos: JHEP 06 (2006) 019, hep-ph/0605083, and references therein.
- [2] Yu.L. Dokshitzer, V.A. Khoze and S.I. Troyan: Int. J. Mod. Phys. **A7** (1992) 1875.
- [3] C.P. Fong and B.R. Webber: Phys. Lett. **B 241** (1990) 255.
- [4] Yu.L. Dokshitzer, V.A. Khoze, S.I. Troyan and A.H. Mueller: Rev. Mod. Phys. **60** (1988) 373-388.
- [5] R. Perez-Ramos & B. Machet: JHEP 04 (2006) 043, hep-ph/0512236.
- [6] OPAL Collab.: Phys. Lett. **B 287** (1992) 401.
- [7] Yu.L. Dokshitzer, V.S. Fadin and V.A. Khoze: Z. Phys **C18** (1983) 37.
- [8] Yu.L. Dokshitzer, V.A. Khoze, A.H. Mueller and S.I. Troyan: “*Basics of Perturbative QCD*”, Editions Frontières, Paris, 1991.
- [9] V.A. Khoze and W. Ochs: Int. J. Mod. Phys. **A12** (1997) 2949.
- [10] C.P. Fong and B.R. Webber: Phys. Lett. **B 229** (1989) 289.